Three-dimensional transition in the buoyancy boundary layer on an evenly heated vertical wall

S. W. Armfield and G. D. McBain

School of Aerospace, Mechanical and Mechatronic Engineering
Sydney University, New South Wales, 2006 AUSTRALIA

Abstract

The three-dimensional structure of the thermal boundary layer adjacent to an evenly heated vertical wall with imposed stable background density stratification is investigated using direct numerical simulation. The wall is considered to extend infinitely in the vertical and spanwise directions, with the heating imposed as a constant flux boundary condition. Flow behaviour is determined by a Reynolds number based on the ratio of the boundary flux gradient to the background gradient. For low Reynolds numbers the flow is stable with variation in the wall normal direction only. For Reynolds numbers greater than a critical value the flow is unstable and supports a two-dimensional wave travelling vertically up the plate, in the direction of fluid flow. A further increase in Reynolds number sees the generation of a three-dimensional spanwise structure on the two-dimensional travelling wave.

Introduction

Flows generated by the transfer of heat from a vertical wall to an adjacent fluid are known as natural convection flows and occur widely in nature and engineering. The rate of heat transfer is strongly dependent on the character of the flow, that is whether it is laminar or turbulent, with turbulent natural convection boundary layer flows having heat transfer rates several times that of a laminar natural convection boundary layer. The transition from laminar to turbulent flow is believed to occur via the generation of rapidly growing three-dimensional waves associated with an initial two-dimensional transition, although the mechanism is not fully understood. In this paper the onset of three-dimensional travelling waves is investigated for the case of an infinite plate having a uniform heat flux, subjected to a stable linear background temperature stratification. For a constant Prandtl number the behaviour of this flow is determined by the ratio of the horizontal temperature gradient imposed at the plate, and the background stable vertical temperature gradient. Below a critical value of this control parameter the flow is steady, one-dimensional and independent of the control parameter. Above a critical value the flow is two-dimensional and oscillatory, exhibiting waves travelling in the vertical direction. A further increase in the control parameter leads to a spanwise, three-dimensional, structure super-imposed on the two-dimensional travelling waves.

The governing equations for this flow are the three-dimensional Navier–Stokes equations with the Oberbeck–Boussinesq approximation for buoyancy, together with a temperature transport equation,

$$u_t + uu_x + vu_y + wu_z = -p_x + \nu(u_{xx} + u_{yy} + u_{zz}), \quad (1)$$

$$v_t + uv_x + vv_y + wv_z = -p_y + \nu(v_{xx} + v_{yy} + v_{zz}) + g\beta T, \quad (2)$$

$$w_t + uw_x + vw_y + ww_z = -p_z + \nu(w_{xx} + w_{yy} + w_{zz}), \quad (3)$$

$$u_x + v_y + w_z = 0, \quad (4)$$

$$T_t + uT_x + vT_y + wT_z + v\Gamma_s = \alpha(T_{xx} + T_{yy} + T_{zz}), \quad (5)$$

where u, v and w are the velocity components in the directions x, y and z respectively, with x the horizontal direction, y the vertical and z the spanwise, t is the time, p the pressure, β, α and ν are the coefficients of thermal expansion, thermal diffusivity and kinematic viscosity respectively and g is the acceleration due to gravity. The temperature is represented as the sum of a background temperature $\overline{T}$ and a perturbation temperature T. The background temperature is assumed to be x and z independent and linear with $\overline{T}_y = \Gamma_s$ a positive constant. The domain is $-\infty < y < \infty, -\infty < z < \infty, 0 \leq x < \infty$, with boundary conditions,

$$u = v = w = 0, \ T_x = -\Gamma_w \quad \text{on} \quad x = 0, \quad (6)$$

$$u, v, w, T \to 0 \quad \text{as} \quad x \to \infty. \quad (7)$$

A one-dimensional steady analytic solution may be found for this flow. Under the assumption that $v = V(x)$ and $T = \Theta(x)$, the governing equations reduce to,

$$0 = \nu V_{xx} + g\beta\Theta, \quad (8)$$

$$V\Gamma_s = \alpha\Theta_{xx}, \quad (9)$$

with the solution,

$$V(x) = \sqrt{2}\Gamma_w \left(\frac{g\beta\alpha^3}{\nu\Gamma_s^3} \right)^{1/4} \times \ldots$$

$$\exp\left\{ -\left(\frac{g\beta\Gamma_s}{4\alpha\nu} \right)^{1/4} x \right\} \sin\left\{ \left(\frac{g\beta\Gamma_s}{4\alpha\nu} \right)^{1/4} x \right\}, \quad (10)$$

$$\Theta(x) = \Gamma_w \left(\frac{g\beta\Gamma_s}{4\alpha\nu} \right)^{-1/4} \times \ldots$$

$$\exp\left\{ -\left(\frac{g\beta\Gamma_s}{4\alpha\nu} \right)^{1/4} x \right\} \cos\left\{ \left(\frac{g\beta\Gamma_s}{4\alpha\nu} \right)^{1/4} x \right\}. \quad (11)$$

This suggests the appropriate dimensional velocity, length and temperature scales for this problem are,

$$U = \sqrt{2}\Gamma_w \left(\frac{g\beta\alpha^3}{\nu\Gamma_s^3} \right)^{1/4}$$

$$H = \left(\frac{4\alpha\nu}{g\beta\Gamma_s} \right)^{1/4},$$

$$\Delta T = \Gamma_w H.$$

Using these quantities to non-dimensionalise (1) to (5) above gives,

$$u_t + uu_x + vu_y + wu_z = -p_x + \frac{1}{Re}(u_{xx} + u_{yy+u_{zz}}), \quad (12)$$

$$v_t + uv_x + vv_y + wv_z = -p_y + \frac{1}{Re}(v_{xx} + v_{yy} + v_{zz}) + \frac{2}{Re}T, \quad (13)$$

$$w_t + uw_x + vw_y + ww_z = -p_z + \frac{1}{Re}(w_{xx} + w_{yy} + w_{zz}), \quad (14)$$

$$u_x + v_y + w_z = 0, \tag{15}$$

$$T_t + uT_x + vT_y + \frac{2v}{RePr} + wT_z = \frac{1}{RePr}(T_{xx} + T_{yy} + T_{zz}), \tag{16}$$

where all quantities are now non-dimensional, the Reynolds number $Re = \frac{UH}{v} = \frac{2\Gamma_w}{\Gamma_s Pr}$ and the Prandtl number $Pr = \frac{v}{\alpha}$. The Reynolds number can also be expressed in terms of a Grashof number $Gr = \frac{g\beta\Delta T H^3}{v^2} = \frac{4\Gamma_w}{\Gamma_s Pr}$ as $Re = \frac{Gr}{2}$, and thus the Reynolds number is also a Grashof number. The boundary conditions for the non-dimensional quantities are,

$$u = v = w = 0, \; T_x = -1 \quad \text{on} \quad x = 0, \tag{17}$$

$$u, v, w, T \rightarrow 0 \quad \text{as} \quad x \rightarrow \infty. \tag{18}$$

The stability of the one-dimensional flow, given by (10) and (11) has been investigated using two-dimensional linear stability analysis employing a Laguerre collocation scheme. The stability analysis has provided the critical Reynolds number, and other properties, and has been shown to accurately predict the behaviour of a full nonlinear solution obtained via a two-dimensional direct numerical solution [7, 8]. At $Pr = 7$, the critical Reynolds number for the onset of an oscillatory solution consisting of two-dimensional travelling waves was found to be $Re_{cr} \simeq 8.6$.

The heat flux boundary condition solution given above is similar to that of the vertical slot with different temperatures on the walls and a uniform vertical gradient, which exhibits boundary layers near either wall, investigated by Elder [4]. The stability of these temperature boundary conditions flows has been examined by Bergholz [2], Christov & Homsy [3], and that of the stratified fluid near a single wall by Gill & Davey [5].

The transition to turbulence in thermal boundary layers is associated with the generation of three-dimensional structures within the boundary layer. Surprisingly however, very few investigations of the three-dimensional stability properties of vertical natural convection boundary layers have been carried out. The definitive experiment was performed by Jaluria & Gebhart [6] for the boundary layer on a vertical plate heated by a constant heat flux. A transverse ribbon near the leading edge was vibrated to trigger instabilities in both the streamwise and spanwise directions; the spanwise structures led to double vortex structures aligned with the streamwise flow during the early stages of transition. The wave number of the spanwise structures was found to be determined by the lateral length scales present in the ribbon itself; however these structures were clearly present and were unstable in the sense that their amplitude increased downstream. The flow associated with the heat flux boundary condition combined with a stable background temperature gradient, investigated here, is considered to be an ideal flow for the further investigation of three-dimensional transition.

In this paper a full numerical nonlinear three-dimensional solution will be obtained using an unsteady Navier–Stokes solver. The results are consistent with those of McBain & Armfield [7] in that they show that, with increasing Re, the initial instability is a two-dimensional travelling wave. A further increase in Reynolds number then leads to a three-dimensional spanwise structure.

Results and Discussion

The equations given above are solved in the domain $0 \leq x \leq X, 0 \leq y \leq Y, 0 \leq z \leq Z$ with initial conditions;

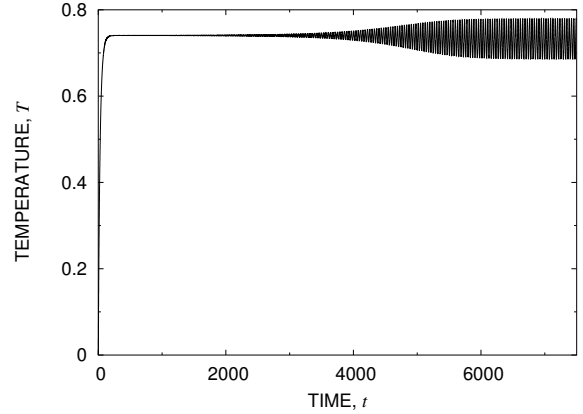$$u = v = w = T = 0, \quad \text{at all} \quad x, y, z \quad \text{and} \quad t = 0; \tag{19}$$

Figure 1: Temperature time series for $Re = 9$

boundary conditions on $x = 0, X$;

$$u = v = w = 0, \; T_x = -1 \quad \text{on} \quad x = 0, \tag{20}$$

$$u_x = v = w = T_x = 0 \quad \text{on} \quad x = X; \tag{21}$$

with periodic boundary conditions on $y = 0, Y, z = 0, Z$;

$$\cdot|_{y=Y} = \cdot|_{y=0}, \; \cdot|_{z=Z} = \cdot|_{z=0}, \tag{22}$$

for variables u, v, w, T

A second order fractional step Navier–Stokes solver defined on a non-staggered rectangular grid is used. Time integration is accomplished using an Adams–Bashforth scheme for the non-linear terms and Crank–Nicolson for the viscous and diffusion terms. All spatial terms are discretised using centred second order differences. Continuity is enforced and pressure obtained using a pressure correction equation. All the discrete equations are inverted using a pre-conditioned conjugate gradient solver. The three-dimensional solver is similar to a two-dimensional solver that has been used for the investigation of natural convection flow for a number of years [1, 7], and the code may be run in either two- or three-dimensional form.

The results presented in figures 1 to 3 were obtained using the code in two-dimensional form. These results were obtained with the domain $X = 16, Y = 13.84$. The x extent of the domain has been chosen to ensure that the large x boundary conditions do not adversely influence the solution, while the y extent has been chosen to match the most unstable wavelength, based on a linear stability analysis, at $Re = 10$. The grid is uniform in y with $\Delta y = 0.25$ and non-uniform in x with $\Delta x = 0.025$ at $x = 0$ and a maximum stretching of 1.025 in the increasing x direction, giving a grid of 119×55 in x and y. The time step is $\Delta t = 5 \times 10^{-4}$. This grid size and time step has been shown to be fine enough to provide asymptotic second order convergence for this flow.

The temperature time series, shown in figure 1, was obtained with an initial random perturbation added to the temperature field in the range $-.005$ to 0.005. The use of an initial perturbation reduces the time required for the unsteady solution to reach full development; however all other features of the flow, such as frequency, growth rate and fully developed ampltitude, are independent of the initial perturbation. As can be seen the flow shows an inital large growth, associated with the base flow development. A sinusoidal oscillation is then seen to develop, growing slowly, and reaching full development by approximately $t = 7000$. The early stages of growth of the sinusoidal oscillation and the frequency are accurately predicted
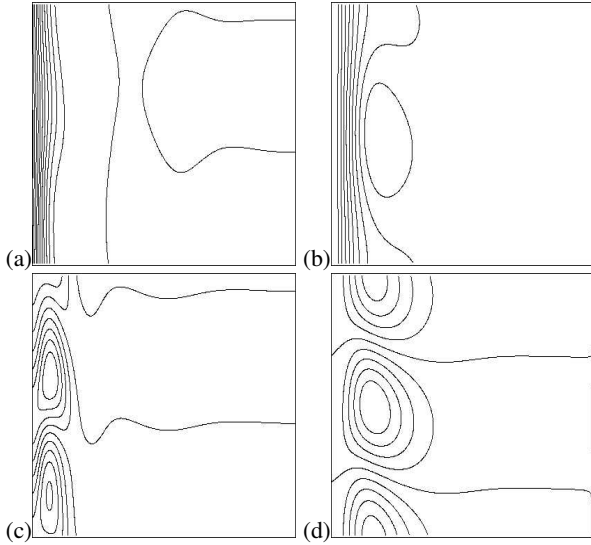
Figure 2: Two-dimensional temperature (a,c) and stream-function (b,d) contours for $Re = 9$; total temperature and stream-function shown in (a,b) and difference from streamwise mean shown in (c,d).

by the linear stability analysis [7], while the final amplitude is determined by nonlinear effects.

Figure 2 shows the temperature and stream-function contours for the $Re = 9$ flow, where the wave structure is clearly seen in both fields. The waves travel vertically with a wave velocity of 0.38—approximately the same as the speed of the critical mode in linear theory. The difference from the streamwise mean is also plotted, clearly showing the wave structure of the perturbation.

Figure 3 shows the temperature contours for the cases $Re = 19$ and $Re = 20$, also obtained with the code in two-dimensional form. Once again the travelling wave structure of the flow is clear, with a noticable increase in amplitude when compared to the $Re = 9$ results. It is also clear that nonlinear effects have also increased as evidenced by the strong asymmetry seen in the waves.

Results obtained with the code in three-dimensional form are shown in figures 4 and 5. These results were obtained on the domain $X = 16, Y = 13.84, Z = 16$. Once again the x extent of the domain was chosen to ensure large x boundary effects did not adversely influence the flow, the y extent was chosen to match the domain used for the two-dimensional results given above. The z extent was chosen arbitrarily and will be discussed below. The grid used has $\Delta x = 0.1, \Delta y = 1.0, \Delta z = 1.0$ with stretching in the increasing x direction of 1.1 and timestep $\Delta t = 2 \times 10^{-3}$. This considerably coarser grid and larger time step, than those used for the two-dimensional simulations, was required to ensure reasonable computation times.

Figure 4 shows temperature contours obtained with the three-dimensional code on constant x and z planes for $Re = 19$. The constant z plane result clearly shows a travelling wave structure, while the constant x result shows no spanwise variation indicating that the solution is two-dimensional. This solution may be compare directly to the equivalent two-dimensional solution shown in figure 3(a) where it is seen that the wave structure is nearly identical. The $Re = 19$ result is therefore a genuinely two-dimensional flow, and it is clear that relatively coarse grid and time step used for the three-dimensional solution is having only a small effect on the overall flow charater.
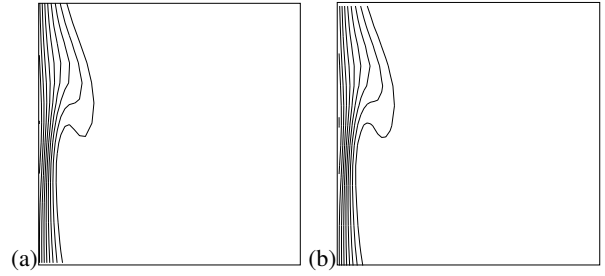

Figure 3: Temperature contours for $Re = 19$, (a), and $Re = 20$, (b) obtained with two-dimensional code.
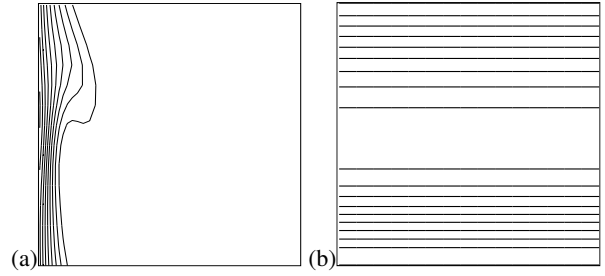

Figure 4: Temperature contours for $Re = 19$ shown on $z = Z/2$ (a), and $x = 0.1$ (b) obtained with three-dimensional code.

Figure 5 shows temperature contours obtained with the three-dimensional code on constant x and z planes for $Re = 20$. The constant z plane result again shows a travelling wave structure, while the constant x plane result now shows a spanwise structure. The flow has clearly undergone a three-dimensional transition between $Re = 19$ and $Re = 20$ and is now exhibiting a wave structure in both the y and z directions. Once again the combined y and z wave structure is travelling vertically. It is interesting to note that the amplitude of the wave as seen in the constant z plane results has reduced from $Re = 19$ to $Re = 20$, and also in comparison to the two-dimensional $Re = 20$ result shown in figure 3(b).

Figure 6 contains the fourier power spectra of time series for the two- and three-dimensional solutions for $Re = 20$. For consistency in this case both solutions were obtained on the same, coarse, grid used for the three-dimensional simulation. Both solutions have a dominant frequency of approximately 0.02, however there are considerable differences in the structure of the two power spectra. The three-dimensional signal is marginally lower in amplitude at frequency 0.02, and considerably lower at the first harmonic, frequency 0.04. Additionally the three-dimensional signal shows a low frequency mode, at approximately 0.002, that is not seen at all in the two-dimensional signal. The three-dimensional signal also shows
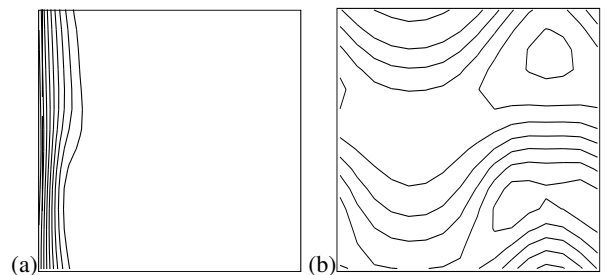

Figure 5: Temperature contours for $Re = 20$ shown on $z = Z/2$ (a), and $x = 0.1$ (b) obtained with three-dimensional code.
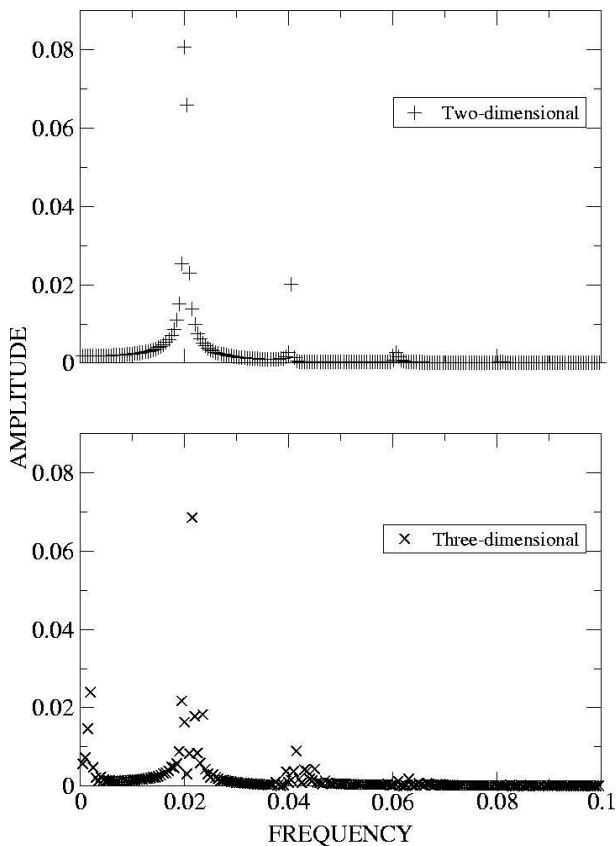
Figure 6: Fourier power spectra of temperature time series for two-dimensional and three-dimensional solutions for $Re = 20$

additional modes close to 0.02 and 0.04 that are not present in the two-dimensional result. The lower amplitude of the three-dimensional signal at 0.02 and 0.04 is associated with the reduced amplitude of the wave seen in the temperature contours, noted above, and is very likely to be a result of the transfer of energy to the spanwise mode, leading to the hypothesis that the three-dimensional transition is associated with a nonlinear transfer of energy from the base two-dimensional mode to the spanwise mode. A single measure of the effect of the travelling waves is the Nusselt number, defined as the mean ratio of the heat transfer coefficient to that prevailing under the base flow. The Nusselt number for the two-dimensional flow at $Re = 20$ is approximately 3% greater than that for the three-dimensional flow, again with both solutions obtained on the coarse mesh used for the three-dimensional simulation. The reduction in Nusselt number seen with the three-dimensional flow is again believed to be a result of the reduced amplitude of the 0.02 and 0.04 frequency modes.

Conclusions

The flow generated by a constant temperature gradient boundary condition on a vertical plate with constant stable background vertical temperature gradient has been found very useful for the investigation of stability and transition in natural convection boundary layers. The sub-critical flow is one-dimensional, with no variation in the y and z directions, allowing the use of parallel flow stability analysis techniques. Direct numerical simulations may be carried out on a reduced domain using periodic boundary conditions in the y and z directions.

The results obtained by McBain & Armfield [7] demonstrated that accurate information about the behaviour of the super-critical flow could be obtained via linear stability analysis. This

provided the critical Reynolds number for transition to oscil-latory two-dimensional flow, as well as information about the wave-length and velocity of the fully nonlinear super-critical flow. The three-dimensional results presented above have shown that the initial transition is genuinely two-dimensional, with a further increase in Reynolds number required to generate a three-dimensional, spanwise, transition.

The results presented here indicate that the critical Reynolds number for three-dimensional transition is between $Re = 19$ and $Re = 20$. These results were obtained for a domain with span-wise extent approximately equal to the resolved vertical wave-length, and it is not immediately clear that this will be the crit-ical spanwise wave-length. The use of a finite domain with pe-riodic boundary conditions does limit the resolvable modes to those with wavelengths that are an integral divisor of the do-main size, and some care must be taken to examine a number of domains to determine critical values. Some initial tests with smaller and larger spanwise extent domains have indicated that the critical spanwise mode has a wave-length approximately equal to that of the base two dimensional streamwise mode, as shown here, giving support to these results, although more work is required to verify this hypothesis.

Acknowledgements

References

[1] Armfield, S. W. and Patterson, J. C., Wave properties of natural convection boundary layers, *J. Fluid Mech.*, **239**, 1992, 195–211.

[2] Bergholz, R. F., Instability of steady natural convection flow in a vertical fluid layer, *J. Fluid Mech.*, **84**, 1978, 743–768.

[3] Christov, C. I. and Homsy, G. M., Nonlinear dynamics of two-dimensional convection in a vertically stratified slot with and without gravity modulation, *J. Fluid Mech*, **430**, 2001, 335–360.

[4] Elder, J. W., Laminar free convection in a vertical slot, *J. Fluid Mech*, **23**, 1965, 77–98.

[5] Gill, A. E. and Davey, A., Instabilities of a buoyancy driven system, *J. Fluid Mech*, **35**, 1969, 776–798.

[6] Jaluria, Y. and Gebhart, B., An experimental study of nonlinear disturbance behaviour in natural convection, *J. Fluid Mech.*, **61**, 1973, 337–365.

[7] McBain, G. D. and Armfield, S. W., Instability of the buoyancy boundary layer on an evenly heated vertical wall. *J. Fluid Mech*, submitted.

[8] McBain, G. D. and Armfield, S. W., Linear stability of natural convection on an evenly heated vertical wall, this conference.